Published in final edited form as:

DNA Repair (Amst). 2016 May ; 41: 16–26. doi:10.1016/j.dnarep.2016.03.003.

Nonhomologous end joining of complex DNA double-strand breaks with proximal thymine glycol and interplay with base excision repair

Mohammed Almohaini[1,5], **Sri Lakshmi Chalasani**[1,5], **Duaa Bafail**[1], **Konstantin Akopiants**[1], **Tong Zhou**[1], **Steven M. Yannone**[2], **Dale A. Ramsden**[3], **Matthew C.T. Hartman**[4], and **Lawrence F. Povirk**[1,*]

[1]Department of Pharmacology and Toxicology, Massey Cancer Center, Virginia Commonwealth University, Richmond, VA 23298

[2]Life Sciences Division, Lawrence Berkeley Laboratory, Berkeley, CA 94720

[3]Lineberger Comprehensive Cancer Center, Department of Biochemistry and Biophysics, University of North Carolina, Chapel Hill, NC 27599

[4]Department of Chemistry, Massey Cancer Center, Virginia Commonwealth University, Richmond VA 23298

Abstract

DNA double-strand breaks induced by ionizing radiation are often accompanied by ancillary oxidative base damage that may prevent or delay their repair. In order to better define the features that make some DSBs repair-resistant, XLF-dependent nonhomologous end joining of blunt-ended DSB substrates having the oxidatively modified nonplanar base thymine glycol at the first (Tg1), second (Tg2), third (Tg3) or fifth (Tg5) positions from one 3′ terminus, was examined in human whole-cell extracts. Tg at the third position had little effect on end-joining even when present on both ends of the break. However, Tg as the terminal or penultimate base was a major barrier to end joining (>10-fold reduction in ligated products) and an absolute barrier when present at both ends. Dideoxy trapping of base excision repair intermediates indicated that Tg was excised from Tg1, Tg2 and Tg3 largely if not exclusively after DSB ligation. However, Tg was rapidly excised from the Tg5 substrate, resulting in a reduced level of DSB ligation, as well as slow concomitant resection of the opposite strand. Ligase reactions containing only purified Ku, XRCC4, ligase IV and XLF showed that ligation of Tg3 and Tg5 was efficient and only partially XLF-dependent, whereas ligation of Tg1 and Tg2 was inefficient and only detectable in the presence of XLF. Overall, the results suggest that promoting ligation of DSBs with proximal base damage may be an important function of XLF, but that Tg can still be a major impediment to repair, being relatively

*Corresponding author, LPOVIRK@vcu.edu, Lawrence F Povirk, VCU Massey Cancer Center, 401 College St, Richmond, VA 23298-0035.

[5]These authors contributed equally to this work.

present address: CinderBio, Berkeley, CA 94720

resistant to both trimming and ligation. Moreover, it appears that base excision repair of Tg can sometimes interfere with repair of DSBs that would otherwise be readily rejoined.

Graphical abstract

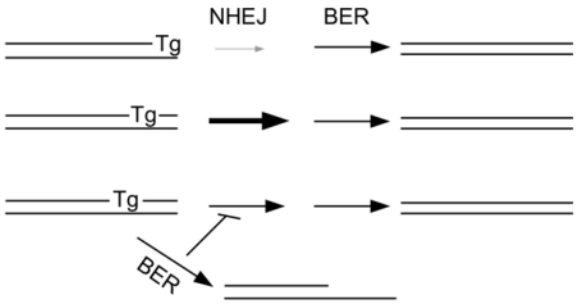

1. INTRODUCTION

Because of the track structure of ionizing radiation, oxidative damage to DNA often occurs in clusters, and this clustering is largely responsible for the formation of double-strand breaks (DSBs) [1–4]. DSBs induced by densely ionizing radiation such as carbon ions are repaired more slowly and less completely that those induced by γ-rays [5], an effect that most likely reflects at least in part the greater chemical complexity of these breaks. Track modeling studies suggest that on average, each DSB induced by γ-rays includes ~2.8 individual oxidative modifications of DNA [4], implying that a large fraction if not a majority DSBs will have at least one additional proximal lesion. For high-LET radiation, which is a major concern for both long-term space travel and charged particle-based radiotherapy, both the prevalence and the complexity of complex DSBs will be even greater. Previous work with DSB substrates containing proximal abasic sites or 8-oxoguanine [6–9], as well as studies with ^{125}I-induced DSBs [7], suggest that lesions near DSB termini can in some cases significantly impair end joining, but that the degree of inhibition is dependent on both the nature of the lesion and its position.

Complex radiation-induced DSBs will comprise random combinations of strand breaks and oxidative base lesions, and while an infinite number of such combinations are possible, the nonplanar base lesion 5,6-dihydroxy dihydrothymine, or thymine glycol (Tg) is a particularly likely candidate for conferring repair resistance. Tg is the predominant form of pyrimidine damage, rivaled only by hydroxyhydantoin [10], and unlike 8-oxoguaine, the primary form of purine damage, Tg disrupts base stacking and blocks replication [11]. To assess the potential of Tg to confer resistance to DSB repair, end joining of defined DSBs with a proximal Tg was examined in a cell extract-based system. The results suggest that Tg in certain positions close enough to a DSB end can evade excision repair and impose a substantial and in some cases an absolute barrier to classical NHEJ.

2. MATERIALS AND METHODS

2.1 Materials

Whole-cell extracts were prepared from confluence-arrested XLF-deficient Bustel fibroblasts [12] as described [13,14]. HCT116 cell extracts were made similarly, except that that growth medium was replaced with medium containing 0.5% serum when the cells reached 50% confluence, and cells were harvested 5 days later. Recombinant His6-tagged XLF and tyrosyl-DNA phosphodiesterase (TDP1) were expressed in E. coli and purified by nickel-affinity chromatography and monoQ FPLC [14]. Mutations were introduced using QuickChange kit (Qiagen). Artemis nuclease [15], X4L4 complex [16] and Ku [17] were produced in baculovirus-infected insect cells. Recombinant human endoIII homologue (hNTH) [18] was kindly provided by Dr. David Pederson, University of Vermont and was stored in small aliquots at −80°C. Tg-containing oligonucleotides were obtained from Midland Certified Reagents, with structural verification by mass spectrometry. Unmodified oligomers were from Integrated DNA Technologies and other enzymes were from New England Biolabs.

2.2 Substrates

Plasmid pUC19 (34 μg) was cut with BstAPI and KasI and the larger 2.6-kb fragment was agarose gel-purified and electroeluted. The 18-mer ATGCGGATCGCGTTGTCT (50 pmoles), either unmodified or with Tg as the 3′-terminal base, was 5′-^{32}P end-labeled with T4 polynucleotide kinase (PNK) in a volume of 10 μl. After inactivation for 3 min at 90°C, it was annealed to 50 pmole of the 21-mer pAGACAACGCGATCCGCATATG by heating to 80°C followed by slow cooling to 10°C, resulting in a duplex with a 3-base -ATG 3′ overhang that is complementary to the -CAT 3′ overhang of the BstAPI site (Fig. 1). Thus, 8 pmole of the duplex was ligated to 2 pmole of the BstAPI/KasI fragment by treatment with 2,400 units T7 DNA ligase for 2 hr at 25°C in 130 μl of the buffer provided by the vendor (66 mM Tris-HCl, 10 mM $MgCl_2$, 1 mM ATP, 1 mM dithiothreitol, 7.5% polyethylene glycol, pH 7.6). Under these conditions, blunt-end ligation by T7 ligase is negligible [19], so that the dominant product was a double-length plasmid joined tail-to-tail at the KasI sites, with the labeled duplex linked to each end (Fig. 1A). This product was cut with SmaI and the final 2.4-kb substrate with one modified and one unmodified blunt end was gel-purified. Substrates with Tg as the second base (terminal sequence -TTGC-Tg-C), third base (-TTG-Tg-CT) or fifth base (-T-Tg-GTCT) from the 3′ end, were similarly constructed. For substrates harboring 5′-proximal Tg, similar duplexes were prepared but with 5′ radiolabel on the Tg-containing 21-mer, in which the 5′-terminal sequence was changed to TC-Tg-GAACG- or C-Tg-CGAACG-.

2.3 End joining reactions

Reactions in extracts contained 50 mM triethanolammonium acetate pH 7.5, 1 mM ATP, 1 mM dithiothreitol, 50 μg/ml BSA, 1.3 mM magnesium acetate and dNTPs (or ddNTPs) at 100 μM each. Typically, a 16-μl reaction contained 10 μl of extract, resulting in a final concentration of 8 mg/ml protein, 66 mM potassium acetate and 16% glycerol, and an effective Mg^{++} concentration of 1 mM (taking into account 0.3 mM EDTA from the extract). Buffer components were first mixed with cell extract at 22°C. Recombinant proteins (XLF

and/or Artemis) were then added, followed immediately by the substrate (20 ng). The reaction was again mixed by pipeting, and placed in a 37°C water bath, usually for 6 h. Samples were then deproteinized as described (13), ethanol-precipitated in the presence of 1 μl GlycoBlue coprecipitant (Invitrogen), cut with NdeI and PstI (20 units each) for 3 hr in 40 μl of NEB CutSmart buffer (50mM potassium acetate, 20 mM Tris-acetate, 10 mM magnesium acetate, 100 μg/ml BSA, pH 7.9) and analyzed on 20% polyacrylamide DNA sequencing gels. Storage phosphor screens were exposed to frozen polyacrylamide gels for 40 hr, and images were analyzed with ImageQuant 5.1 software. For some experiments, samples were treated with E. coli endonuclease III (EndoIII) to cleave Tg-containing products. For treatment prior to restriction cleavage, half of each deproteinized, precipitated sample was treated with 20 units EndoIII for 2 hr at 37°C in 20 μl of the buffer provided by the vendor (20 mM Tris-HCl, 1 mM EDTA, 1 mM dithiothreitol, pH 8), followed by EndoIII inactivation for 20 min at 65°C and addition of NdeI, PstI and CutSmart buffer. In other experiments, after NdeI/PstI cleavage, sodium acetate was added to 0.3 M along with a 44-base oligomer (100 nM) complementary to the expected Tg-containing strand of a blunt-end ligation product. The sample was denatured at 90°C and then annealed by slow cooling to 10°C. Samples were then ethanol-precipitated and treated with EndoIII as above, and again precipitated prior to denaturing gel electrophoresis.

2.4 Reactions with purified proteins

Reactions with purified NHEJ proteins contained 25 mM Tris-HCl pH 8, 100 mm NaCl, 0.1 mM EDTA, 50 μg/ml BSA, 0.05% Triton X-100, 2 mM DTT, 5% polyethylene glycol (MW ~ 8000), 5 mM $MgCl_2$ and 0.1 mM ATP [20]. Protein concentrations were 10 nM Ku, 40 nM X4L4 (based on a 1:1 complex of XRCC4 and ligase IV) and 50 or 100 nM XLF. Samples including NHEJ proteins were prepared on ice and reactions were initiated by simultaneous addition of $MgCl_2$ and ATP. Samples were incubated at 37°C for 30 min, then deproteinized and cut with NdeI and PstI as above.

hNTH was stored in small aliquots at −80°C and was diluted immediately before use in 50 mM Tris-HCl pH 7.5, 150 mM NaCl, 1 mM DTT, 0.005% triton X100, 10% glycerol. hNTH reactions were performed in 20 μl of 25 mM Tris-HCl pH 8, 250 mM potassium glutamate, 1 mM DTT [18] and were incubated for 1 hr at 37°C. In some cases 5 μg/ml recombinant TDP1 was then added and the incubation was continued for 1 hr. DNA was deproteinized by phenol extraction, cut with NdeI, and analyzed on sequencing gels as above. For the substrates with 5′-proximal Tg, samples were incubated with hNTH, denatured and electrophoresed on 36% nondenaturing polyacrylamide gels to assess release of the resulting 1- or 2-base 5′-terminal fragment

3. RESULTS

3.1 NHEJ is tolerant of a substrate containing Tg near a DSB end

Because Tg is a major product of free radical damage to DNA, it will likely often occur at or near the terminus of a radiation-induced DSB. Because Tg is nonplanar, it induces severe distortion in DNA structure [11]. Classical NHEJ, however, is capable of joining mismatched overhangs as well as a variety of other noncomplementary end structures [20–

22]. To determine whether Tg poses a barrier to ligation in the context of NHEJ, internally labeled blunt-ended substrates were constructed (Fig. 1) with Tg as the first, second or third base from the 3′ terminus of one DNA end (Tg1, Tg2 and Tg3, respectively); the opposite end was blunt but unmodified. End joining of these substrates was detected by subsequent cleavage with NdeI and PstI, which release labeled and unlabeled fragments, respectively, from opposite ends of the substrate. For Tg-containing samples, the 19-mer corresponding to unjoined substrate migrates as a doublet, reflecting different stereoisomers of Tg (Fig. 2).

To assess whether Tg was a barrier to NHEJ, each of the four blunt-end substrates was incubated in whole-cell extracts of XLF-deficient Bustel fibroblasts. For the unmodified, blunt-ended substrate, end joining was completely dependent on addition of purified recombinant XLF, and the only detectable products were the expected 44-base head-to-tail and 36-base head-to-head products of direct blunt-end ligation, each of which precisely comigrated with synthetic markers of the same sequence (Fig. 2A, lanes 22–28). Unexpectedly, the Tg3 substrate (lanes 15–21) yielded, in addition to apparent 36- and 44-base products, a third product migrating as a slightly diffuse band above the 36-mer band (labeled as 36Tg). To identify this band, the sample was treated EndoIII, an E. coli base excision repair (BER) enzyme known to excise Tg bases from double-stranded DNA [23]. Treatment of the DNA with EndoIII after incubation in extracts but before NdeI/PstI cleavage (lane 18) eliminated most of this band (Fig. 2C), suggesting that it represents a 36-base head-to-head ligation product in which Tg is still present. This Tg-containing 36-mer migrates more slowly than the unmodified 36-base product, which migrates anomalously fast because it is palindromic and can snap back into a hairpin upon denaturation/renaturation. The Tg apparently disrupts hairpin formation and thereby decreases the electrophoretic mobility, providing a convenient indication of the extent to which head-to-head end joining products still contained the Tg base.

In addition, EndoIII treatment eliminated about half of the 44-base product, suggesting that, as with the 36-base product, Tg was still present in some but not all of the ligated 44-base products. As further confirmation that some of the Tg had been excised and replaced with thymine, the experiment was performed with ddTTP added to the extracts in place of dTTP, to prevent ligation of DNAs from which Tg had been excised. For samples with ddTTP, the faster-migrating unsubstituted 36-base product from Tg3 was largely eliminated, confirming that it arose from excision repair of a Tg-containing ligation product (lane 21). The unmodified and Tg3 substrates yielded approximately the same level of 44-base product (22.1% vs 19.2%, Fig. 2B), and the sum of the Tg-substituted and unsubstituted 36-base products from Tg3 (6.3% and 5.9%, respectively, Fig. 2C) was equal to the yield of single 36-base base product from the unmodified substrate (11.6%, data not shown), indicating that overall, Tg at the third position from a DNA end conferred little or no inhibition of NHEJ.

3.2 Tg as the terminal or penultimate base at the 3′ end of a DSB is a barrier to NHEJ

In contrast to the efficient blunt-end ligation seen with the Tg3 substrate, the Tg1 and Tg2 substrates yielded only a trace of 44-base product, approximately 1–2% of the total substrate or about tenfold less than Tg3 (Fig. 2A, lanes 1–14). Moreover, Tg1 and Tg2 yielded no detectable 36-base head-to-head joining product. These results indicate that Tg as the

terminal or penultimate base constitutes a major barrier to blunt-end ligation in NHEJ when present at one end of a DSB, and an absolute barrier when present at both ends.

One possible mechanism for resolution of such a barrier would be trimming of the Tg by Artemis, an endonuclease that associates with DNA-PK and is activated by that association [24]. As shown previously, there is insufficient Artemis in whole-cell extracts to trim canonical Artemis substrates such as 3′ overhangs of DSBs, but addition of exogenous recombinant Artemis results in nearly complete overhang trimming, culminating in efficient ligation of the trimmed intermediate to an end with a complementary overhang ([25] and Supplemental Fig. 1). In contrast, for the Tg-containing substrates, added Artemis did not detectably increase trimming beyond the low level already seen in the unsupplemented extracts (Fig 2A, lanes 6, 14, 19 and 26). Nevertheless, for the Tg2 substrate only (lane 14), addition of Artemis resulted in a twofold increase in the yield of ligated product (1.48±0.08% vs. 0.77±0.07%, N=3), accompanied by a slight decrease in its length (~2 bases, based on its mobility). These results suggest that Tg near a DSB 3′ terminus can be trimmed by Artemis, albeit inefficiently.

3.3 Ligation of Tg-containing substrates does not require prior Tg removal

For the Tg3 substrate, EndoIII treatment prior to restriction nuclease digestion clearly reduced the yield of 44-base product, but for the Tg1 substrate in particular (Fig. 2A, lane 4), EndoIII appeared to have little effect. Although this result could be explained by a replacement of Tg by normal thymine in all the Tg1 ligation products, an alternative possibility is that only the Tg-containing strand was ligated, and the remaining nick in the opposite strand prevented EndoIII from acting. To assess the presence of Tg without regard to the status of the complementary strand, end joining products generated in extracts containing either dTTP or ddTTP were cut with NdeI and PstI, then denatured, and annealed to an excess of a 44-base oligomer complementary to the expected ligation product of the labeled, Tg-containing strand. The annealed products were finally treated with EndoIII (Fig. 3). Under these conditions, EndoIII reduced the yield of 44-base product from the Tg1 and Tg2 substrates by half, and from the Tg3 substrate by 30%. Thus, the NHEJ machinery was clearly capable of ligating all three Tg-containing substrates, albeit inefficiently, even ligating a 3′-terminal Tg to a blunt end. These results also exclude the possibility that the apparent ligation of Tg1 and Tg2 substrates were the results of contamination with a small fraction of the corresponding unmodified substrates. As expected, EndoIII had no effect on the yield of products from the unmodified substrate. Also, EndoIII does not eliminate the 36Tg product of Tg3 in these experiments because the denaturation/renaturation process converts it to a hairpin structure that is not cleaved by EndoIII.

For all of the Tg-containing substrates, substitution of ddTTP for dTTP likewise reduced the yield of ligation products dramatically, and also eliminated most of the EndoIII-resistant ligation products (Fig. 3); the remainder may be due to some residual dTTP in the extracts. This result shows that Tg was sometimes excised and replaced with thymine, although it does not distinguish whether such replacement occurred before or after blunt-end ligation of the DSB. In the case of the Tg3 substrate, this question was addressed by substituting ddCTP for dCTP during incubation in the extracts. If Tg were either trimmed off by a

nuclease or removed by BER prior to ligation of the DSB, the two 3′-terminal bases attached to it would presumably be lost as well, so that a blunt-end ligation product could only be formed by re-synthesis with dCTP and dTTP. Thus, the finding that ddCTP did not reduce the yield of blunt-end ligation product (Fig. 4A, lane 9 and Fig 4B, lane 8) suggests that most if not all ligations of the Tg3 substrate occurred with Tg still present.

3.4 An initial delay in ligation is dependent on Tg position

To further investigate the order of Tg excision and DSB ligation, samples were taken at various times after addition of substrate to the extract. For the Tg3 substrate, ligated products began to accumulate rapidly after an initial delay of about 30 min, but the Tg-containing 36Tg fragment accumulated much faster than the thymine-containing 36-base fragment (Fig. 4A and 4C). These data are consistent with a mechanism wherein ligation preceded Tg removal and replacement, so that at later times continuing ligation was approximately balanced by slow excision of Tg from the ligated product, resulting in a steady-state level of the 36-base Tg-containing ligation product (36Tg). Thus, this result lends further support to the inference, from ddCTP trapping experiments, that ligation precedes Tg removal and replacement in formation of the unmodified (thymine-containing) 36-base product. There was, however, an initial delay of about 30 min before a significant level of end joining products appeared (Fig. 4C). For the Tg1 substrate, a longer delay of nearly 2 hr was seen (Fig. 4D). However, when extract and substrate were preincubated for 2 hr in the absence of XLF, end joining began immediately upon XLF addition, suggesting that there was some prejoining process that did not require XLF but that either proceeded more slowly with the Tg1 substrate, or was only essential for the Tg1 substrate.

3.5 Tg at the fifth base from a 3′ end is subject to BER that interferes with end joining

Unexpectedly, whereas Tg at the third position from a blunt 3′ end had at most a small effect on the extent of end joining, a substrate with Tg at the fifth position (Tg5) showed a much lower level of end joining, yielding only 3.5±0.8% head-to-tail ligations, about sixfold lower than the unmodified substrate (Fig. 5A). This reduced ligation was accompanied by the rapid accumulation of a 14-base fragment corresponding to apparent cleavage at the site of the Tg, presumably reflecting glycoslylase-mediated BER. Within 30 min, this shorter fragment accounted for nearly 40% of total initial substrate (Fig. 5B). Thus, although previous results indicate that gaps of 1–2 bases on partially complementary overhangs are efficiently patched and ligated in these extracts [14], it appears that the recessed end resulting from Tg removal was not efficiently filled in. Nevertheless, the Tg5 substrate, like Tg3, generated 36-base head-to-head products of which half contained thymine in place of Tg (Fig. 5A), suggesting that once end joining has occurred, Tg5 and Tg3 are equally susceptible to moderately efficient BER. Thus, the massive accumulation of cleaved but unpatched Tg5 molecules, in contrast to the near absence of analogous intermediates for Tg3, probably reflects excision of Tg from Tg5 DSB ends which had not been ligated. This view is supported by agarose gel electrophoresis of the products of end joining in extracts, which confirmed that Tg5 was joined to a lesser extent than Tg3 (Supplemental Fig. 2). Excision of Tg from Tg5 yields a 4-base oligonucleotide that would likely dissociate spontaneously to leave a 5-base-recessed 3′ terminus. To test this possibility, the Tg5 substrate was incubated in extract, deproteinized and treated with exonuclease-deficient Klenow fragment to fill in the putative recessed 3′

terminus before NdeI/PstI cleavage (Fig. 5C). For the 15-minute sample, virtually all of the 14-mer was extended to a 19-mer (lane 3), indicating that it had a 3′-hydroxyl terminus (the 20-mer represents addition of an extra nucleotide to the blunt end by this enzyme [26]). Thus, the lack of fill-in in the extracts was not due to either a blocked 3′ terminus or loss of the 5′ overhang. However, Klenow-mediated fill-in of the 6-hr sample gave a more diverse spectrum of 15- to 20-base fragments, suggesting that the 5′ overhang resulting from BER was subject to very slow exonucleolytic resection (Fig. 5C, lane 5).

To distinguish whether position-dependent differences in susceptibility to BER were due to BER substrate specificity or to substrate accessibility, the Tg substrates were treated with human EndoIII homologue (hNTH) in the absence of other proteins. At high hNTH concentrations, the Tg5 and Tg3 substrates yielded prominent shorter fragments whose mobility was consistent with the expected 3′-deoxyribose phosphate (dRp)-terminated 14-mer or 12-mer, respectively, that would be produced by the Tg glycosylase and lyase activities of hNTH, along with a trace of the 3′-phosphate fragment corresponding to 3′-dRp hydrolysis (Fig. 6A and Supplemental Fig. 3). Subsequent treatment with TDP1 converted most of the remaining putative 3′-dRp termini to 3′-phosphate termini, as expected [27]. However, titrations with limiting hNTH showed that Tg was much more susceptible to cleavage in Tg5 than in Tg3, where only a minority of Tg sites were cleaved even at the highest hNTH concentrations (Fig. 6B). Furthermore, there was no detectable Tg cleavage in Tg1 or Tg2 (Supplemental Fig. 3). Thus, the observed interference with NHEJ by BER in Tg 5 but not the other substrates, is consistent with the substrate specificity of hNTH.

3.6 Proximal Tg produces similar inhibitory effects on NHEJ in extracts of tumor cells

Bustel fibroblasts are ideal for end joining studies because when grown to confluence arrest, they produce extracts with particularly robust repair activity, and because their XLF deficiency facilitates verification that joining reflects classical NHEJ. However, in terms of implications for radiotherapy, it is also important to assess repair in tumor cells. End joining of Tg substrates in extracts of HCT116 colorectal cancer cells, although less efficient overall than in Bustel extracts, showed similar specificities (Fig. 7). Tg at the terminal and penultimate positions severely impacted end joining, while Tg at the third position from the 3′ terminus had little effect. As in the Bustel extracts, Tg at the fifth position showed extensive cleavage and reduced end joining, reflecting likely interference by BER.

3.7 Purified Ku, X4L4 and XLF are sufficient for end joining of Tg substrates

In whole-cell extracts, end joining of normal as well as Tg-containing substrates was strictly dependent on XLF, indicating that it represents canonical NHEJ. However, the results do not exclude the possibility that proteins other than the core NHEJ factors, might be required for some substrates. Previous work showed that significant ligation of compatible DNA ends can be carried out by purified X4L4 and Ku without XLF [16]. Similarly, significant head-to-tail ligation of the unmodified blunt-ended substrate, as well as the Tg5 substrate, was detected in reactions containing only Ku and X4L4 (Fig. 8A, 44-base fragment), and XLF addition increased the yield only about twofold. However, ligation of Tg3 was more strongly dependent on XLF, with XLF omission decreasing the yield approximately tenfold (Fig. 8B). Ligation of Tg1 and Tg2 was detected only in the presence of XLF, but because the

yield was only ~0.3% in both cases, the exact degree of stimulation by XLF was difficult to gauge. Clearly, however, Tg5 was ligated at least as efficiently as Tg3 by the combination of purified Ku, X4L4 and XLF. Thus, the finding that in extracts Tg5 was joined less efficiently than Tg3, was likely not due to a greater intrinsic resistance to ligation, but instead due to interference by BER.

3.8 Proximal Tg in the 5′-terminal strand confers comparable inhibition of NHEJ

Analogous substrates harboring 5′-proximal Tg were also constructed, to assess the possible effect on NHEJ. When placed in the 3′-terminal strand, Tg conferred much greater inhibition at the second position from the terminus than at the third position; therefore, substrates with Tg at the second and third position from the 5′ terminus, designated 5′ Tg2 and 5′ Tg3, respectively, were constructed, with the radiolabel on the 5′-terminal phosphate (Fig. 9). Qualitatively, results were similar to those for 3′-proximal Tg in that Tg at the second position was more inhibitory than at the third position, but the difference was not as dramatic, less than twofold. Nevertheless, like its 3′ analogue, the 5′ Tg2 substrate yielded no detectable head-to-head ligation products, while 5′ Tg3 yielded only a trace. Both 5′ Tg2 and 5′ Tg3 also yielded small amounts of shorter unidentified products (~22–25 bases) that were not seen with either the unmodified 5′-end-labeled substrate or any of the substrates with 3′-proximal Tg. While this result would be consistent with resection of several bp from a DSB end before ligation, such resection could not have included the proximal Tg, as in that case the 5′ label would also have been lost.

Treatment of the 5′ Tg substrates with purified hNTH alone revealed that both of them were less susceptible to cleavage than the (3′-proximal) Tg5 substrate, although more susceptible than Tg3 (Fig. 9D). The fact that, in end joining experiments (Fig. 9B), the intensity of the 17-mer band corresponding to the intact substrate did not show a substantial reduction upon incubation of the 5′-proximal Tg substrates in the extracts, suggests that there was relatively little Tg cleavage prior to ligation in these substrates.

4. DISCUSSION

In mammalian cells, repair of DSBs induced by ionizing radiation, as judged either by pulsed-field gel electrophoresis of cellular DNA [28] or by the assembly and dissolution of γH2AX foci [29], is typically biphasic. Whereas the majority of breaks are rejoined within 1 hour, the remaining 10–20% require several additional hours. Although most of the slow component of repair likely represents DSBs in heterochromatin [30], the finding that DSBs formed by high-LET radiation are also rejoined rather slowly [5], suggests that the chemical complexity of a DSB is an additional factor in increasing the time required for its repair. Slower repair in turn could increase the probability that DSB ends become physically separated, leading to lethal or carcinogenic chromosome breaks and rearrangements.

Complex DSBs can reasonably be assumed to comprise random combinations of fragmented sugars and any of a multitude of oxidatively modified bases, spread over 10–20 bp of DNA [1,31,32]. Once terminal blocking groups, primarily 3′-phosphates and 3′-phosphoglycolates, are removed, religation of otherwise compatible ends may still be prevented by base damage, especially structure-distorting base lesions very close to the

termini. Tg, one of the most common oxidative lesions in DNA [10], is nonplanar, resulting in severe local perturbation of DNA structure [11], potentially rendering DSBs resistant to repair. Although in principle these damaged ends could be trimmed off by the NHEJ-associated Artemis nuclease [24,33], previous work indicates that presence of Tg near a DSB end does not promote such trimming, but on the contrary inhibits trimming of structures that would otherwise be favored Artemis substrates, such as 3′ overhangs [25]. On the other hand X4L4 can ligate diverse nonmatching ends that are not substrates for other ligases, and its tolerance for mismatched ends is enhanced by XLF [20,21]. To determine the tolerance of NHEJ for modified structures that would occur in complex, free radical-mediated DSBs, joining of ends harboring Tg at various distances from the 3′ terminus was examined in Bustel whole-cell extracts. End joining of all substrates in this system is completely dependent on the presence of XLF as well and DNA-PKcs, and is blocked by a DNA-PKcs inhibitor [13,14,34], suggesting that it reflects exclusively classical NHEJ. Moreover, inasmuch as these extracts can carry out all steps of NHEJ with very high efficiency (as much as 30–50% of free ends rejoined), they likely contain ample concentrations of the core NHEJ proteins Ku, DNA-PKcs, X4L4 and XLF, and possibly additional factors that remain to be identified.

Tg as the third base from a blunt end (Tg3 substrate) had only a small inhibitory effect on ligation of blunt ends by the combination of X4L4, XLF and Ku, and almost no effect on ligation in extracts. The significant proportion of head-to-head ligations derived from this substrate indicates that such ancillary damage was tolerated even when present at both ends of a break. Although Tg in this substrate was eventually replaced with thymine, presumably via BER, DSB ligation usually if not always preceded Tg excision, as indicated by the rapid accumulation of ligated Tg-containing products (Fig. 4). In the unligated substrate, there appeared to be minimal processing by BER, as there was little accumulation of the 2-base-shorter fragment that would result from BER in the presence of ddTTP.

In contrast, Tg at the fifth base from the terminus was rapidly excised, resulting in a dramatic accumulation of truncated fragments even in the absence of ddTTP. This excision was associated with, and was likely the cause of, a reduced yield of end-joined products, as compared with Tg3 or the unmodified substrate. Most likely, the 4-base fragment between the excision site and the DSB end would spontaneously dissociate to leave a 5-base-recessed 3′ end. Although this recessed end was hydroxyl-terminated, in extracts it was not extended to any measurable extent, even though the generation of Tg-free ligation products from the Tg1 and Tg2 substrates suggest that the extracts are competent for BER-associated gap filling (presumably by polβ), while experiments with other substrates suggest that the NHEJ-associated polλ is present and functional [35]. Instead, the 5′ overhang appears to be slowly shortened, in some cases producing a truncated blunt end. Overall, the results suggest that, at least in extracts, BER can interfere significantly with NHEJ when a modified base is far enough from an end to be a favorable BER substrate. Experiments with purified hNTH, in which the Tg5 substrate showed robust Tg cleavage, also support this view. In contrast to these results, Covo et al. [6] showed that, during NHEJ of a DSB with one blunt end and one 2-base-recessed end in a transfected substrate, the recessed end was usually filled in. It is not clear which factor (2-base vs. 5-base gap, different cell lines, extracts vs. transfection) is responsible for the apparent difference in results.

On the other hand, experiments with both extracts and purified hNTH indicate that the unligated Tg1, Tg2 and Tg3 substrates were poor substrates for BER, as judged by the low levels of cleavage at Tg sites. In extracts, this was true even when ddTTP was added to trap any transient BER intermediates (Fig. 3). Since the Tg1 and Tg2 products were also poor substrates for NHEJ-mediated ligation as well as for Artemis-mediated trimming (Fig. 2), DSBs of this type when formed in cells could be quite persistent, increasing the probability of either misjoining to the end of a different DSB, or of a collision with a replication fork or transcription complex. This is particularly true for breaks with base damage at both ends. With the Tg1 and Tg2 substrates, there was not under any condition any detectable head-to-head ligation of such DSBs. In S and G2 phase, a persistent, terminally blocked DSB end could be 5′-resected by Mre11 and CtIP and thereby channeled into repair by homologous recombination [36]. However, the damaged 3′ end would still have to be resolved at some point in order to prime the synthesis required for completion of HRR [37]. Mre11/CtIP may also carry out more limited 5′ resection in G1 [38,39], perhaps exposing enough undamaged 3′ overhang to promote trimming by Artemis, finally yielding an end more compatible with NHEJ.

Nevertheless, for DSBs with damage at just one end, there was measurable ligation of even a terminal Tg, both by XLF-complemented extracts and by the combination of purified Ku, X4L4 and XLF. The sensitivity of the ligated products to EndoIII excludes the possibility that this result could have been due to contamination of Tg oligomers with undamaged DNA. It remains possible that additional proteins or environmental properties in the cell allow this reaction to proceed more efficiently in vivo than in vitro, and if so, facilitating such ligations of DNA ends that contain base damage may be one of the most important functions of XLF. Although XLF stimulates X4L4-mediated ligation of all substrates, ligation of Tg3 appeared to be more strongly dependent on XLF than ligation of an unmodified substrate (Fig. 8).

End joining of DSBs accompanied by proximal base damage has been examined previously, with somewhat disparate results. In two studies, 8-oxoguanine was incorporated as the penultimate base on the recessed 3′ terminus of a DSB with a cohesive 5′ overhang. Datta et al. [7] reported that this modification dramatically reduced end joining in whole-cell extracts of HeLa, WI38 and M059K cells, and that the ligated products still contained 8-oxoG. However, Dobbs et al. [8] found that although 8-oxoG in this position completely blocked ligation by purified X4L4, it had only a modest effect on end joining in HeLa cell extracts. With respect to BER, 8-oxoG was a poor substrate when placed within 4 bases of a 3′ end or within 6 bases of a 5′ end [8]. The two studies were in agreement that an abasic lesion in the same 3′-penultimate position was a more severe barrier to end joining than was 8-oxoG. A more recent study, wherein defined substrates were tranfected into cells and the products analyzed by high-throughput sequencing, showed that 8-oxoG as the 5′-terminal base of a 4-base 5′ overhang was well-tolerated during NHEJ, and that ligation of the DSB usually preceded replacement of 8-oxoG with normal guanine [9]. Using T4 ligase, Dobbs et al obtained a similar, somewhat counterintuitive result: that 8-oxoG was better tolerated within the cohesive overhang of a DSB than in the nearby surrounding sequence [8]. Unlike 8-oxoG, Tg is nonplanar and thus more disruptive of DNA structure. Nevertheless, all studies

appear to agree that modification of the 3′-penultimate base pair at a DSB has a strong tendency to disrupt ligation for NHEJ.

Datta et al. [7,40,41] also examined the molecular structure as well as repairability of site-specific DSBs induced by an ^{125}I-labeled triplex-forming oligonucleotide, as a model of high-LET radiation. Proximal base lesions (i.e., glycosylase-sensitive sites) were detected in at least 50% of each strand in the vicinity of the DSB, and a comparable number of abasic sites (E. coli endonuclease IV-sensitive sites) were detected as well. Moreover, HeLa extracts were able to repair only a small fraction of the ^{125}I-induced DSBs. Taken together, the results of all these studies suggest that oxidative base lesions are very common in high-LET DSBs and that they can be a severe impediment to repair by classical NHEJ, at least as it occurs in whole-cell extracts.

Previous work has indicated that BER can render clustered base damage and abasic sites more lethal than they would be without repair, by converting these lesions to even more toxic DSBs [4]. The present work suggests that BER can also increase lethality of some complex DSBs, by interfering with what would otherwise be efficient religation, while at the same time failing to remove base lesions very near the DSB ends, where they most strongly impede rejoining.

Supplementary Material

Refer to Web version on PubMed Central for supplementary material.

Acknowledgments

We thank David Pederson for providing hNTH. This work was supported by grants CA40615 and CA166264 from the National Cancer Institute, USDHHS, and by Pilot Project Grant A35320 from Massey Cancer Center.

References

1. Hall, EJ.; Giaccia, AJ. Radiobiology for the Radiologist Wolters Kluwer/Lippincott, Williams & Wilkins. 2012.
2. Ward JF. Biochemistry of DNA lesions. Radiat Res Suppl. 1985; 8:S103–11. [PubMed: 3867077]
3. Goodhead DT. Initial events in the cellular effects of ionizing radiations: Clustered damage in DNA. Int J Radiat Biol. 1994; 65:7–17. [PubMed: 7905912]
4. Georgakilas AG, O'Neill P, Stewart RD. Induction and repair of clustered DNA lesions: What do we know so far? Radiat Res. 2013; 180:100–109. [PubMed: 23682596]
5. Shibata A, Conrad S, Birraux J, Geuting V, Barton O, Ismail A, Kakarougkas A, Meek K, Taucher-Scholz G, Lobrich M, Jeggo PA. Factors determining DNA double-strand break repair pathway choice in G2 phase. Embo j. 2011; 30:1079–1092. [PubMed: 21317870]
6. Covo S, de Villartay JP, Jeggo PA, Livneh Z. Translesion DNA synthesis-assisted non-homologous end-joining of complex double-strand breaks prevents loss of DNA sequences in mammalian cells. Nucleic Acids Res. 2009
7. Datta K, Purkayastha S, Neumann RD, Pastwa E, Winters TA. Base damage immediately upstream from double-strand break ends is a more severe impediment to nonhomologous end joining than blocked 3′-termini. Radiat Res. 2011; 175:97–112. [PubMed: 21175352]
8. Dobbs TA, Palmer P, Maniou Z, Lomax ME, O'Neill P. Interplay of two major repair pathways in the processing of complex double-strand DNA breaks. DNA Repair (Amst). 2008; 7:1372–1383. [PubMed: 18571480]

9. Waters CA, Strande NT, Pryor JM, Strom CN, Mieczkowski P, Burkhalter MD, Oh S, Qaqish BF, Moore DT, Hendrickson EA, Ramsden DA. The fidelity of the ligation step determines how ends are resolved during nonhomologous end joining. Nat Commun. 2014; 5:4286. [PubMed: 24989324]
10. Evans MD, Dizdaroglu M, Cooke MS. Oxidative DNA damage and disease: Induction, repair and significance. Mutat Res. 2004; 567:1–61. [PubMed: 15341901]
11. Aller P, Rould MA, Hogg M, Wallace SS, Doublie S. A structural rationale for stalling of a replicative DNA polymerase at the most common oxidative thymine lesion, thymine glycol. Proc Natl Acad Sci U S A. 2007; 104:814–818. [PubMed: 17210917]
12. Buck D, Malivert L, de Chasseval R, Barraud A, Fondaneche MC, Sanal O, Plebani A, Stephan JL, Hufnagel M, Le Deist F, Fischer A, Durandy A, de Villartay JP, Revy P. Cernunnos, a novel nonhomologous end-joining factor, is mutated in human immunodeficiency with microcephaly. Cell. 2006; 124:287–299. [PubMed: 16439204]
13. Baumann P, West SC. DNA end-joining catalyzed by human cell-free extracts. Proc Natl Acad Sci U S A. 1998; 95:14066–14070. [PubMed: 9826654]
14. Akopiants K, Zhou RZ, Mohapatra S, Valerie K, Lees-Miller SP, Lee KJ, Chen DJ, Revy P, de Villartay JP, Povirk LF. Requirement for XLF/Cernunnos in alignment-based gap filling by DNA polymerases λ and μ for nonhomologous end joining in human whole-cell extracts. Nucleic Acids Res. 2009; 37:4055–4062. [PubMed: 19420065]
15. Povirk LF, Zhou T, Zhou R, Cowan MJ, Yannone SM. Processing of 3′-phosphoglycolate-terminated DNA double strand breaks by artemis nuclease. J Biol Chem. 2007; 282:3547–3558. [PubMed: 17121861]
16. Nick McElhinny SA, Snowden CM, McCarville J, Ramsden DA. Ku recruits the XRCC4-ligase IV complex to DNA ends. Mol Cell Biol. 2000; 20:2996–3003. [PubMed: 10757784]
17. Campisi J. From cells to organisms: Can we learn about aging from cells in culture? Exp Gerontol. 2001; 36:607–618. [PubMed: 11295503]
18. Galick HA, Kathe S, Liu M, Robey-Bond S, Kidane D, Wallace SS, Sweasy JB. Germ-line variant of human NTH1 DNA glycosylase induces genomic instability and cellular transformation. Proc Natl Acad Sci U S A. 2013; 110:14314–14319. [PubMed: 23940330]
19. Doherty AJ, Ashford SR, Subramanya HS, Wigley DB. Bacteriophage T7 DNA ligase. overexpression, purification, crystallization, and characterization. J Biol Chem. 1996; 271:11083–11089. [PubMed: 8626651]
20. Gu J, Lu H, Tsai AG, Schwarz K, Lieber MR. Single-stranded DNA ligation and XLF-stimulated incompatible DNA end ligation by the XRCC4-DNA ligase IV complex: Influence of terminal DNA sequence. Nucleic Acids Res. 2007; 35:5755–5762. [PubMed: 17717001]
21. Tsai CJ, Kim SA, Chu G. Cernunnos/XLF promotes the ligation of mismatched and noncohesive DNA ends. Proc Natl Acad Sci U S A. 2007; 104:7851–7856. [PubMed: 17470781]
22. Waters CA, Strande NT, Wyatt DW, Pryor JM, Ramsden DA. Nonhomologous end joining: A good solution for bad ends. DNA Repair (Amst). 2014; 17:39–51. [PubMed: 24630899]
23. D'Ham C, Romieu A, Jaquinod M, Gasparutto D, Cadet J. Excision of 5,6-dihydroxy-5,6-dihydrothymine, 5,6-dihydrothymine, and 5-hydroxycytosine from defined sequence oligonucleotides by escherichia coli endonuclease III and fpg proteins: Kinetic and mechanistic aspects. Biochemistry. 1999; 38:3335–3344. [PubMed: 10079077]
24. Ma Y, Pannicke U, Schwarz K, Lieber MR. Hairpin opening and overhang processing by an Artemis/DNA-dependent protein kinase complex in nonhomologous end joining and V(D)J recombination. Cell. 2002; 108:781–794. [PubMed: 11955432]
25. Mohapatra S, Yannone SM, Lee SH, Hromas RA, Akopiants K, Menon V, Ramsden DA, Povirk LF. Trimming of damaged 3′ overhangs of DNA double-strand breaks by the metnase and artemis endonucleases. DNA Repair (Amst). 2013; 12:422–432. [PubMed: 23602515]
26. Clark JM, Joyce CM, Beardsley GP. Novel blunt-end addition reactions catalyzed by DNA polymerase I of escherichia coli. J Mol Biol. 1987; 198:123–127. [PubMed: 3323527]
27. Interthal H, Chen HJ, Champoux JJ. Human Tdp1 cleaves a broad spectrum of substrates, including phosphoamide linkages. J Biol Chem. 2005; 280:36518–36528. [PubMed: 16141202]

28. Stenerlow B, Karlsson KH, Cooper B, Rydberg B. Measurement of prompt DNA double-strand breaks in mammalian cells without including heat-labile sites: Results for cells deficient in nonhomologous end joining. Radiat Res. 2003; 159:502–510. [PubMed: 12643795]
29. Leatherbarrow EL, Harper JV, Cucinotta FA, O'Neill P. Induction and quantification of gamma-H2AX foci following low and high LET-irradiation. Int J Radiat Biol. 2006; 82:111–118. [PubMed: 16546909]
30. Goodarzi AA, Noon AT, Deckbar D, Ziv Y, Shiloh Y, Löbrich M, Jeggo PA. ATM signaling facilitates repair of DNA double-strand breaks associated with heterochromatin. Mol Cell. 2008; 31:167–177. [PubMed: 18657500]
31. Ward JF. DNA damage produced by ionizing radiation in mammalian cells: Identities, mechanisms of formation, and reparability. Prog Nucleic Acid Res Mol Biol. 1988; 35:95–125. [PubMed: 3065826]
32. Hutchinson F. Chemical changes induced in DNA by ionizing radiation. Prog Nucleic Acids Res Mol Biol. 1985; 32:115–154.
33. Yannone SM, Khan IS, Zhou R, Zhou T, Valerie K, Povirk LF. Coordinate 5′ and 3′ endonucleolytic trimming of terminally blocked blunt DNA double-strand break ends by artemis nuclease and DNA-dependent protein kinase. Nucleic Acids Res. 2008; 36:3354–3365. [PubMed: 18440975]
34. Povirk LF, Zhou RZ, Ramsden DA, Lees-Miller SP, Valerie K. Phosphorylation in the serine/threonine 2609–2647 cluster promotes but is not essential for DNA-dependent protein kinase-mediated nonhomologous end joining in human whole-cell extracts. Nucleic Acids Res. 2007; 5:3869–3878. [PubMed: 17526517]
35. Lee JW, Blanco L, Zhou T, Bebenek K, Garcia-Diaz M, Kunkel TA, Wang Z, Povirk LF. Implication of DNA polymerase lambda in alignment-based gap filling for nonhomologous DNA end joining in human nuclear extracts. J Biol Chem. 2004; 279:805–811. [PubMed: 14561766]
36. Sartori AA, Lukas C, Coates J, Mistrik M, Fu S, Bartek J, Baer R, Lukas J, Jackson SP. Human CtIP promotes DNA end resection. Nature. 2007; 450:509–514. [PubMed: 17965729]
37. Povirk LF. Processing of damaged DNA ends for double-strand break repair in mammalian cells. ISRN Molecular Biology. 2012; 2012:345805.
38. Averbeck NB, Ringel O, Herrlitz M, Jakob B, Durante M, Taucher-Scholz G. DNA end resection is needed for the repair of complex lesions in G1-phase human cells. Cell Cycle. 2014; 13:2509–2516. [PubMed: 25486192]
39. Quennet V, Beucher A, Barton O, Takeda S, Lobrich M. CtIP and MRN promote non-homologous end-joining of etoposide-induced DNA double-strand breaks in G1. Nucleic Acids Res. 2011; 39:2144–2152. [PubMed: 21087997]
40. Datta K, Jaruga P, Dizdaroglu M, Neumann RD, Winters TA. Molecular analysis of base damage clustering associated with a site-specific radiation-induced DNA double-strand break. Radiat Res. 2006; 166:767–781. [PubMed: 17067210]
41. Datta K, Neumann RD, Winters TA. Characterization of a complex 125I-induced DNA double-strand break: Implications for repair. Int J Radiat Biol. 2005; 81:13–21. [PubMed: 15962759]

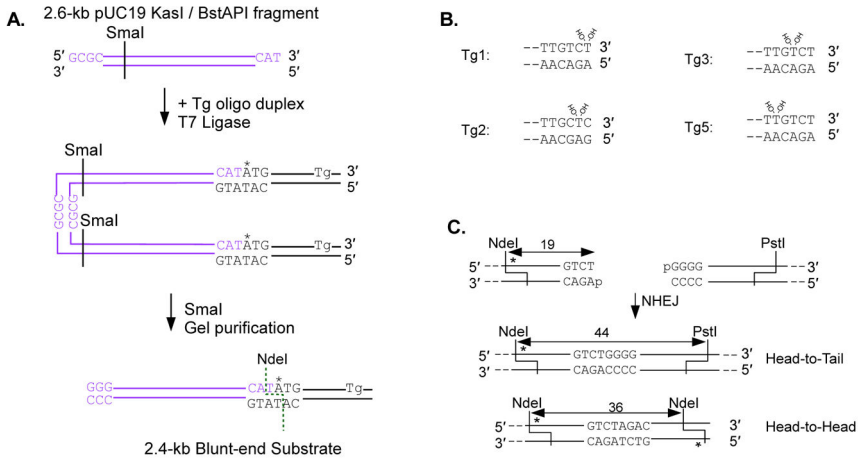

Figure 1.

Tg-containing DSB substrates. A. Construction of modified substrates from short, end-labeled (*) Tg-containing duplexes and a fragment of pUC19. B. Terminal structures and sequences of the substrates. C. Formation of head-to-tail and head-to-head end joining products, and their detection as fragments of NdeI/PstI cleavage.

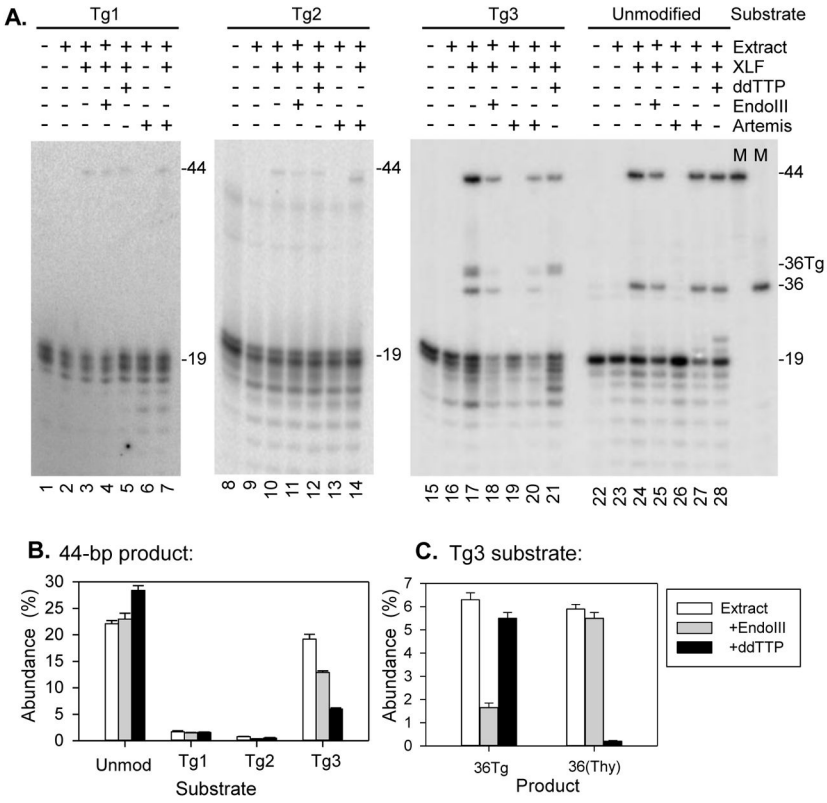

Figure 2.

Effect of Tg on joining of blunt-ended substrates by NHEJ. The indicated site-specifically labeled substrates, either unmodified or containing Tg at the first, second or third position from the terminus of the labeled end, were incubated in XLF-deficient Bustel extracts (or heat-inactivated extracts), supplemented with XLF (100 nM), Artemis (80 nM), and/or ddTTP in place of dTTP as indicated, for 6 hr at 37°C. The samples were deproteinized, in some cases treated with EndoIII, then cut with NdeI and PstI and analyzed on denaturing gels. Lanes marked “M” contain 5′-end-labeled 36- and 44-base oligomers of the sequence expected for blunt-end ligation products. Bar graphs show yield of specific products of the indicated substrates and error bars indicate mean ± SEM for 4 replicate experiments.

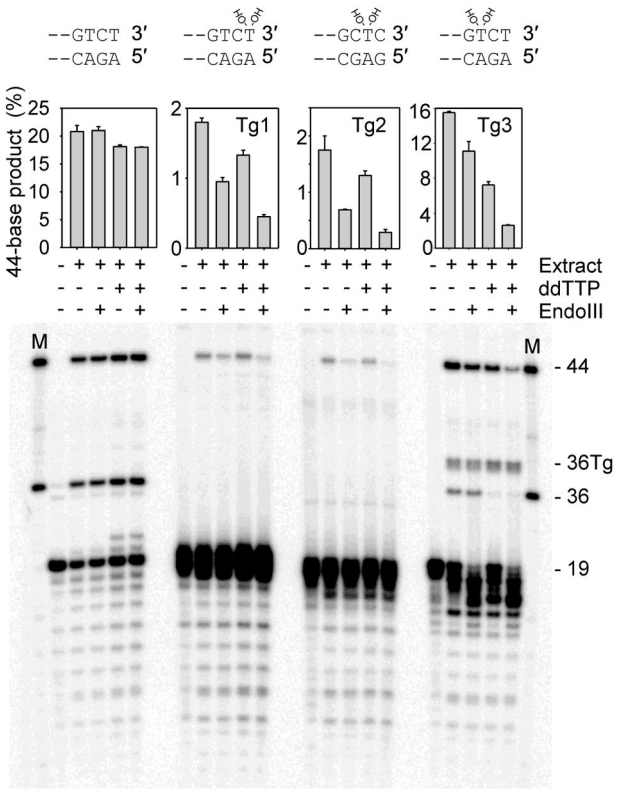

Figure 3.

Presence of Tg in end joining products. Tg-containing or unmodified substrates were incubated for 6 hr in Bustel extracts supplemented with XLF and ddTTP as indicated. Samples were deproteinized and cut with NdeI and PstI, then denatured and annealed to 44-base complements of the expected head-to-tail ligation products and treated (or not) with EndoIII prior to denaturing gel electrophoresis. Bar graphs show the yield of 44-base products in each case (mean ± SEM for 3 independent experiments).

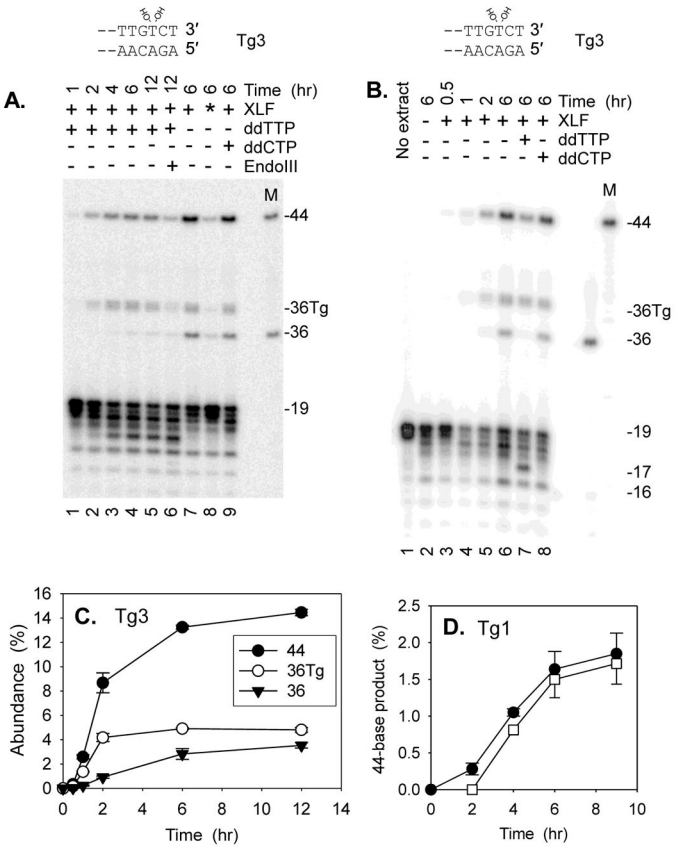

Figure 4.

Time course for Tg3 and Tg1 end joining and effect of dideoxynucleotides. A. and B. Tg3 was incubated in extracts containing ddTTP, ddCTP and/or XLF for the times indicated, then cut with NdeI and PstI and analyzed as in Fig. 2. One sample in (A.) was treated with EndoIII prior to NdeI/PstI cleavage, as in Fig. 2. Asterisk (*) indicates addition of a mutant XLF with an L115A mutation. C. Quantitative analysis of Tg3 ligation in the presence of dNTPs, derived from three replicates of the experiment shown in (B.). D. Time course of formation of end joining for Tg1. The Tg1 substrate was incubated in extracts, with XLF added either at the start of the reaction (●) or after 2 hr incubation (□). Reaction conditions were as in Fig. 2.

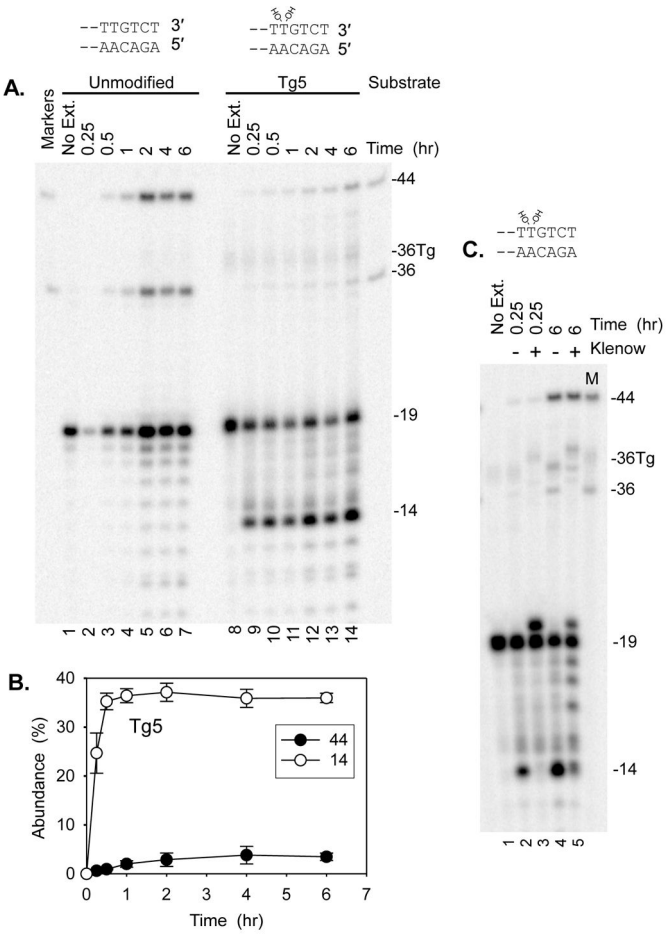

Figure 5.

Interference between BER and end joining of Tg5. A. Either the Tg5 substrate or a corresponding unmodified substrate was incubated in extracts containing XLF for the times indicated, then cut with NdeI and PstI and analyzed as in Fig. 2. B. Quantitative analysis of three experiments with the Tg5 substrate, showing levels of the truncated 14-base fragment or the 44-base head-to-tail end joining product. C. Verification of a recessed 3′-hydroxyl terminus. The Tg5 substrate was incubated in extract for the indicated times, then treated with exonuclease-deficient Klenow fragment prior to NdeI/PstI cleavage. No Ext. = incubation in heat-inactivated extract for 6 hr.

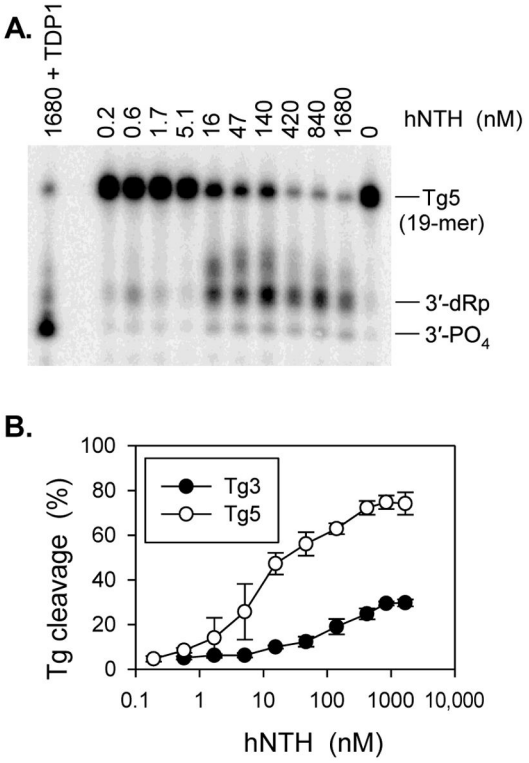

Figure 6.

Tg cleavage by purified hNTH. A. The Tg5 substrate was treated with the indicated concentrations of hNTH for 1 hr, then cut with NdeI prior to denaturing gel electrophoresis. Sample in leftmost lane was also treated with TDP1 to remove 3′-dRp. B. Tg cleavage as a function of hNTH concentration for the Tg3 and Tg5 substrates (mean ± SEM for 3 experiments). The Tg1 and Tg2 substrates showed no detectable cleavage at any hNTH concentration.

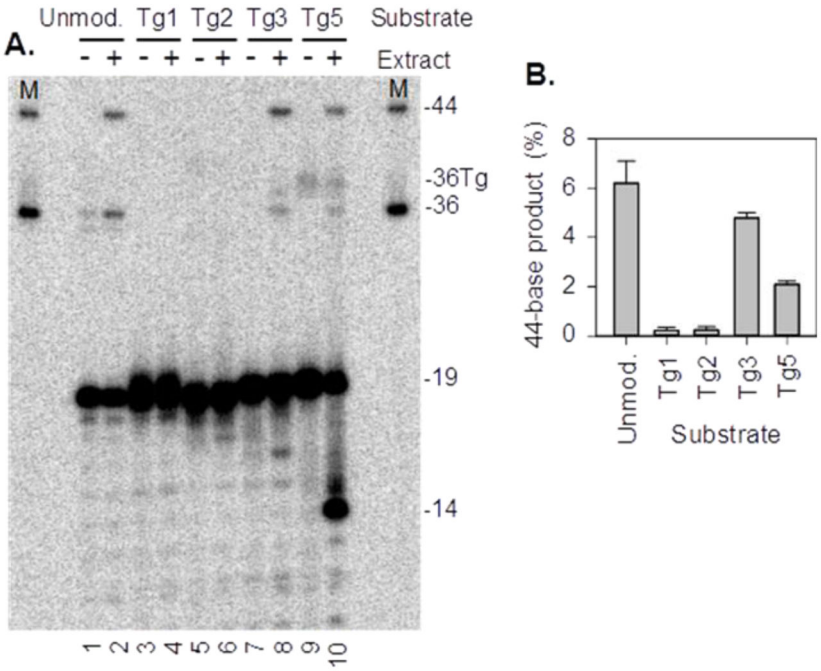

Figure 7.

Effect of 3′-proximal Tg on end joining in HCT116 extracts. The indicated substrates were inbubated in unsupplemented extracts of HCT116 cells and end joining was analyzed as in Fig. 2. **A.** Gel electrophoresis of end joining products. **B.** Pooled data from three replicate experiments showing abundance of the head-to-tail 44-bp product.

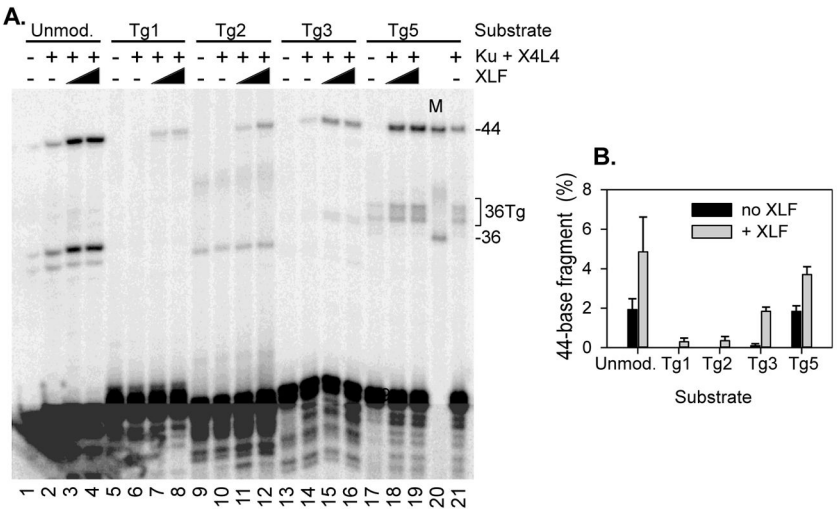

Figure 8.

Ligation of Tg-containing substrates by purified Ku, X4L4 and XLF. A. The indicated substrates were incubated with 10 nM Ku, 40 nM X4L4 and 50 or 100 nM XLF as indicated for 4 hr, then deproteinized and cut with NdeI and PstI and analyzed on a sequencing gel. B. Quantitation of results from 3 independent experiments with 100 nM XLF (mean ± SEM).

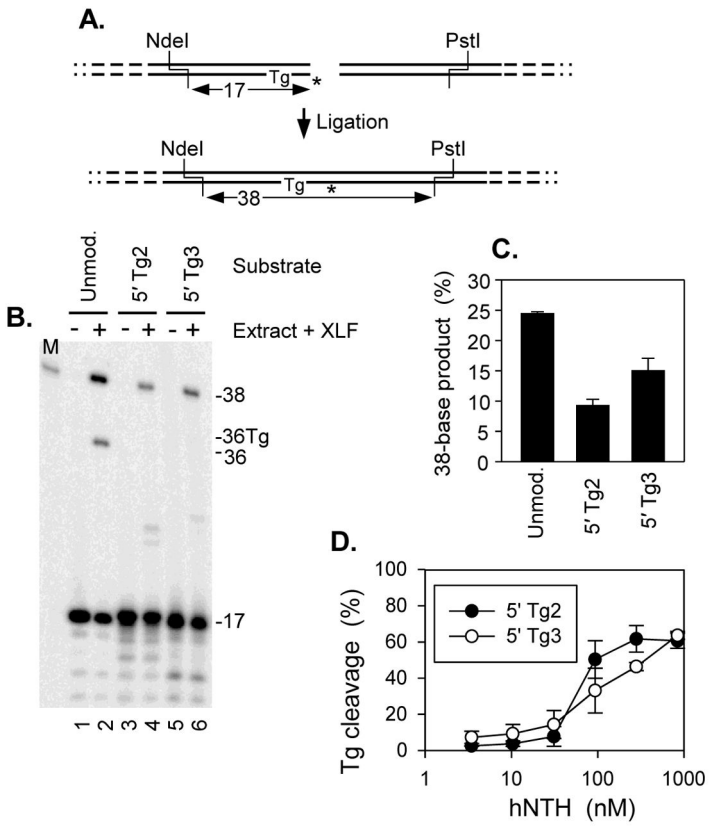

Figure 9.

Effect of 5′-proximal Tg on NHEJ. The blunt-ended substrates shown, with Tg as the second or third base from the 5′ terminus, were incubated for 6 hr in XLF-complemented Bustel extracts. **A.** Substrates and head-to-tail ligation products. The palindromic 36-base head-to-head product is identical to that shown in Fig. 1C, except for terminal sequence. **B.** Denaturing gel analysis of end joining products following cleavage with NdeI and PstI. **C.** Pooled data for formation of head-to-tail products, from 3 independent experiments (mean ± SEM). **D.** Cleavage of 5′-proximal Tg substrates by purified hNTH (mean ± SEM for 3 experiments). Substrates were incubated with the indicated concentrations of hNTH, and release of the 5′-terminal 1- or 2-base fragment was assessed by gel electrophoresis (see Supplemental Fig. 4).